SEMICONDUCTORS

Founded by Ioffe Institute

Published since January 1967

12 issues annually

ISSN: 1063-7826 (print), 1090-6479 (online)

SEMICONDUCTORS is the English translation
of ФИЗИКА И ТЕХНИКА ПОЛУПРОВОДНИКОВ
(FIZIKA I TEKHNIKA POLUPROVODNIKOV)

Published by Ioffe Institute

Saint Petersburg
Ioffe Institute

UDC 621.315.592

Selective growth of GaAs epitaxial layers on a Si substrate by method of vapor-phase epitaxy from the organometallic compounds

© S.O. Slipchenko, V.V. Shamakhov, M.I. Kondratov, A.E. Grishin, M.V. Tokarev, E.V. Fomin, D.N. Nikolaev, A.V. Myasoedov, N.A. Bert, N.A. Pihtin

Ioffe Institute,
St. Petersburg, Russia

E-mail: serghpl@mail.ioffe.ru

Received December 10, 2025
Revised February 13, 2026
Accepted March 10, 2026

Using the method of selective epitaxy the two types of GaAs-structures were grown on Si substrate — with deposition of SiO_2-mask directly on the substrate surface (type 1) and with deposition of SiO_2-mask on the surface of a planar buffer layer of GaAs (type 2). The effect of the structure design on the surface morphology using atomic force microscopy and profilometry, as well as the defects of formed epitaxial layers using scanning and transmission electron microscopy, has been studied. It was demonstrated that the density of the growing-in dislocations was $2.9 \cdot 10^8$ and $2.1 \cdot 10^8\,cm^{-2}$ for the structures of 1 and 2 type, respectively. The RMS surface roughness in the center of the window was 4.87 and 3.26nm for structures of type 1 and 2, respectively.

Keywords: vapor-phase epitaxy, selective epitaxy, silicon substrate, GaAs.

DOI: 10.61011/SC.2026.01.63720.8870

1. Introduction

Currently, there is a high interest in semiconductor heterostructures created by selective epitaxy, the key difference of which is that growth occurs in pre-prepared areas of the wafer, while the remaining part is protected by a passivating mask [1]. Selective epitaxy allows for broader possibilities in controlling the properties of the fabricated heterostructures compared to classical planar epitaxy, in which epitaxial layers have the same properties for the wafer entire surface. A significant part of the research on selective epitaxy technology is related to growth on GaAs or InP [2–5] substrates. For example, in jcite6, the mechanisms of selective growth of GaAs nanogrids obtained by vapor-phase epitaxy from organometallic compounds were investigated. Studies of [3,7,8] have shown the ability to control the properties of the active region formed during selective epitaxy in order to adjust the wavelength of a selected single vertically emitting source. The studies [9,10] cover the results describing the growth features of bulk layers of solid solutions and quantum wells by selective epitaxy in wide windows, demonstrating altered growth mechanisms due to a change in the local misorientation of the epitaxial layer surface.

It should be noted that selective epitaxy technology is an important tool in the engineering of photonic integrated circuits (PIC) [4,11]. If selective epitaxy on $A^{III}B^{V}$ substrates expands the options for controlling the properties of heterostructures, then using this technology with the growth of $A^{III}B^{V}$ light-emitting heterostructures on silicon is a must. This is due to the fact that with monolithic integration, the light-emitting heterostructure should be formed only in the selected local part of PIC, while the rest of PIC should be preserved for the formation of waveguides, dividers, filters and other elements that control optical radiation. In this regard, it is necessary to study the growth features of $A^{III}B^{V}$ structures by selective epitaxy on Si substrates. Currently, there are several approaches used to create light-emitting structures on silicon. One of them is based on the use of constructions involving GaAs buffer structures. These structural elements serve as a transition region between the silicon substrate and the light-emitting structure and provide a lower density of defects in the active region. Another important parameter of selective epitaxy technology is the size of the window where the growth occurs. Within the study, the structures with ultra-wide windows have been selected, which will reduce the requirements for the accuracy of matching between the PIC elements in the future. The article highlights the studies of the general patterns of selective growth of GaAs epitaxial layers (serving as buffers) on a silicon substrate and also outlines the effect of their structure on the main characteristics of surface roughness, defect density, and thickness uniformity.

2. Sample preparation

The structures were grown by vapor-phase epitaxy from organometallic compounds in a vertical reactor type unit „TurboDisc“ (this name is a trademark and can also be used as a technical term). Trimethylgallium was used as a reagent for elements of group III, and arsine was used as a reagent for elements of group V. Hydrogen was used as a carrier vapor.

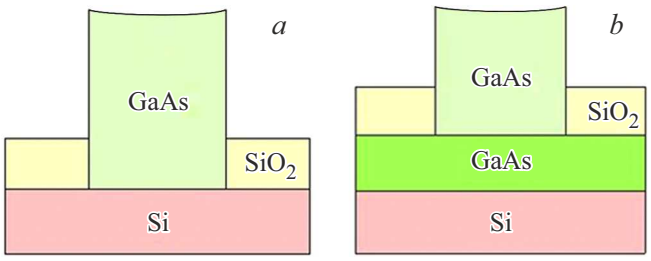

Figure 1. Schematic representation of sample 1 (a) and sample 2 (b).

Two types of samples, differing in their structure, were studied in order to determine the structure effect on the characteristics of the selectively grown layer. General view of the samples is given in Figure 1. For sample 1, selective epitaxy was performed in windows formed in SiO_2 mask deposited directly on Si substrate (Figure 1, a). Sample 2 included a planar GaAs buffer layer grown on a Si substrate where windows were formed for subsequent selective epitaxy (Figure 1, b). Thus, for sample 2, selective growth was carried out in windows formed in the mask SiO_2, deposited on the surface of a planar GaAs buffer layer. In fabrication of samples of both types, a Si (001) substrate with a misorientation 4° in direction [110] was used. SiO_2 film 0.2 μm thick, applied by reactive ion plasma sputtering, was used as a mask. After applying the layer of SiO_2, alternating windows $W = 88\,\mu$m wide and $L = 2870\,\mu$m long with a period of 400 μm were formed in it using lithography and wet etching. A buffer etchant was used. This width of the window was selected because modern PIC technologies allow dealing with multiple tasks at a time, when several projects are deployed on one wafer. This is due to the large area of available Si substrates and silicon-on-insulator wafers and the desire to reduce costs. In this case, the ability to use wide windows significantly simplifies the design process and allows the use of standard libraries of PIC elements. Another aspect — is a decrease of the effect of window/mask interface on the formed $A^{III}B^{V}$ regions. After forming the windows to obtain a sample of type 1, selective growth of GaAs layer was carried out (see Figure 1, a). During the growth process the temperature rose from 400 to 650 °C. For sample 2, at the first stage, a 1.85 μm thick planar GaAs buffer layer was grown on Si substrate. During the growth process of the planar buffer layer, the growth temperature was also increased from 400 to 650 °C, i.e. this buffer was grown similarly to the selectively grown layer in the sample 1. At the second stage, selective growth of GaAs was carried out in the formed windows in SiO_2 layer on the planar GaAs buffer layer at a temperature of 650 °C (Figure 1, b) in order to provide total thickness of the planar buffer layer with the selectively grown part in the window's center, close to the thickness in the window's center of sample 1. All growth was carried out at a reduced reactor pressure of 100 mbar. The molar flux of trimethylgallium for the selective part of both samples was $3.1 \cdot 10^{-5}$ mol/min, and that of arsine was $1.1 \cdot 10^{-3}$ mol/min. The growth rate of GaAs during planar growth on a Si substrate, corresponding to this molar flux of trimelgallium, was 20 nm/min. The hydrogen flow through the reactor was 10 l/min. The samples were then examined using scanning electron microscopy (SEM), atomic force microscopy (AFM), transmission electron microscopy (TEM), and profilometry. SEM-study was made using the microscope JEOL JSM 7001F. AFM studies were performed on microscope NTEGRA (NT-MDT Spectrum Instruments) in intermittent-contact mode using ETALON HA_FM probes. TEM-study was made using the microscope JEM Jeol 2100F. The thickness profile changes were studied using profilometer Ambios XP-1.

3. Results and discussion

In order to generally analyze the growth characteristics at the window/mask interface and the nature of the surface in the window, SEM studies of the samples were carried out (Figure 2). From Figure 2, a, b it is evident that the lateral faces of the studied samples have different shapes. For a sample of type 2 (Figure 2, b), the lateral face corresponds to the plane (111), which is typical for selective epitaxy during growth on GaAs substrate (001). For the sample of type 1 (Figure 2, a) the shape of the lateral face is significantly different. Thus, the lower edge of the layer's lateral surface corresponds to the plane $(11\bar{1})$, the central one — to the plane (110), and the upper one — to the plane (111). The designation of the faces in Figure 2, a corresponds to the conditionally chosen coordinate system, when the structure is observed along the direction $[\bar{1}10]$, and the growth surface corresponds to the plane (001). The determination of the Ga and As polarity of 111 faces, as well as comparison of its effect on the formation of the habit, were not specifically carried out in the study. Based on our findings, (111)A and (111)B faces are featuring a comparable formation rate. For the structures growth the substrate Si (001) with a misorientation of 4° in direction [110] was used. It is assumed that the orientation of the polar faces remains the same for all strip structures on the substrate. From Figure 2, c, d it is evident that SEM images of the sample surfaces, obtained at the same magnification in the center of the window, also have noticeable differences. For sample 1 (Figure 2, c) the surface relief is more distinct than for sample 2 (Figure 2, d). It should be stressed that for sample 1, polycrystalline formation is observed on the surface of the mask, while the mask of sample 2 remains clean. This behavior is due to the fact that in sample 1, the growth of part of GaAs layer is carried out at low temperatures, which results in deposition of part of the material on the mask and further this material becomes the center of crystallization during subsequent growth. In Figure 2, e, a SEM image of the surface for

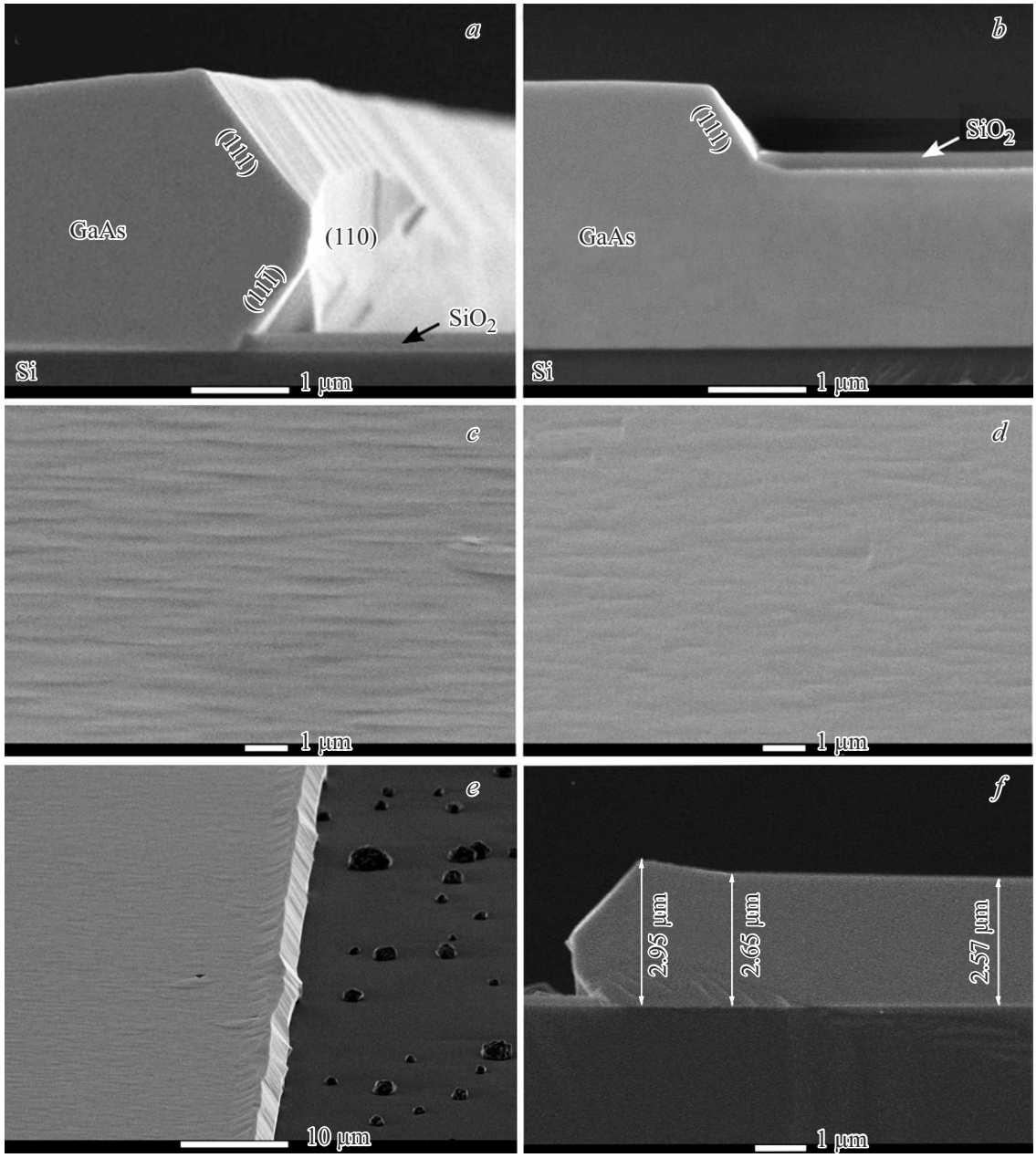

Figure 2. SEM-image of cleavage at the window/mask interface (sample 1 (*a,f*) and sample 2 (*b*)), surface in the window's center (sample 1 (*c*) and sample 2 (*d*)) and surface at the window/mask interface of sample 1 (*e*). The scale mark on the images *a*–*d,f* corresponds to 1 μm, and for the image *e* — 10 μm.

sample 1 at the window/mask interface is presented. The image shows that scattered polycrystals of various sizes are observed on the mask surface, i.e. the entire surface is not covered with a continuous layer of polycrystals. The density of polycrystals on the surface rises towards the central part of the mask between the stripes (this image is not shown in this paper). In sample 2, growth occurs under temperature conditions when the mask remains clean, i.e., all the substance that gets on the mask is desorbed and, due to the concentration gradient in the gas phase, diffuses towards the window. This behavior is typical for selective growth in standard conditions by metal-organic vapor-phase epitaxy on $A^{III}B^{V}$ [12] substrates.

To assess the changes in the thickness of GaAs layer in the window during selective epitaxy, the samples were examined on a profilometer. For each structure, 3 thickness profiles were prescribed for the window width (W) in different parts of it. Figure 3 illustrates the profiles showing the change in GaAs layer thickness for the window width (W) for samples 1 and 2. In the above thicknesses of the selectively grown GaAs layer, the thickness of the mask 0.2 mm was taken into account, since the mask SiO_2 was not

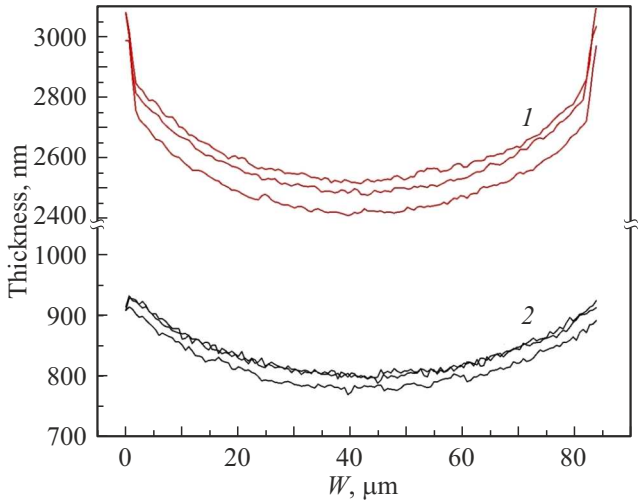

Figure 3. Profiles of variation of the selectively grown GaAs over window width (W): *1* — sample 1, *2* — sample 2.

removed during measurements. For sample 1 the thickness of the selectively grown layer GaAs in the window's center was 2410−2510 nm, and at the edge of the window it was 3000−3100 nm. At the same time, the difference in thickness between the edge and the center of the window was 590 nm. It is also seen that at the window's edge there is an area with a width of ~ 2 microns, in which there is a sharp increase in the thickness of the GaAs layer. This is also clearly visible in SEM-image (Figure 2,*f*). For sample 2, GaAs layer thickness in the center of the window was 780−800 nm, and at the edge of the window 895−925 nm, which gives a thickness variation between the edge and the center of the window of 115−125 nm. It can be seen that the thickness of GaAs layer over the entire width of the window for sample 2, in contrast to sample 1, varies smoothly as it moves from the center of the window to its edge (Figure 3). Today, there are several approaches to the formation of PIC elements. One of them is based on the structure growth in deep windows formed in silicon-on-insulator structures, and the growth of polycrystals on the mask is acceptable, while chemical-mechanical polishing procedure is used to remove them. However, in this case, it is necessary to use additional technological operations to protect and remove the relevant materials, therefore, reducing the density or absence of polycrystals on the surface of the mask is an important goal in the development of selective growth technology. Selective epitaxy is also needed to control the thickness of the active region in order to allow the growth of a number

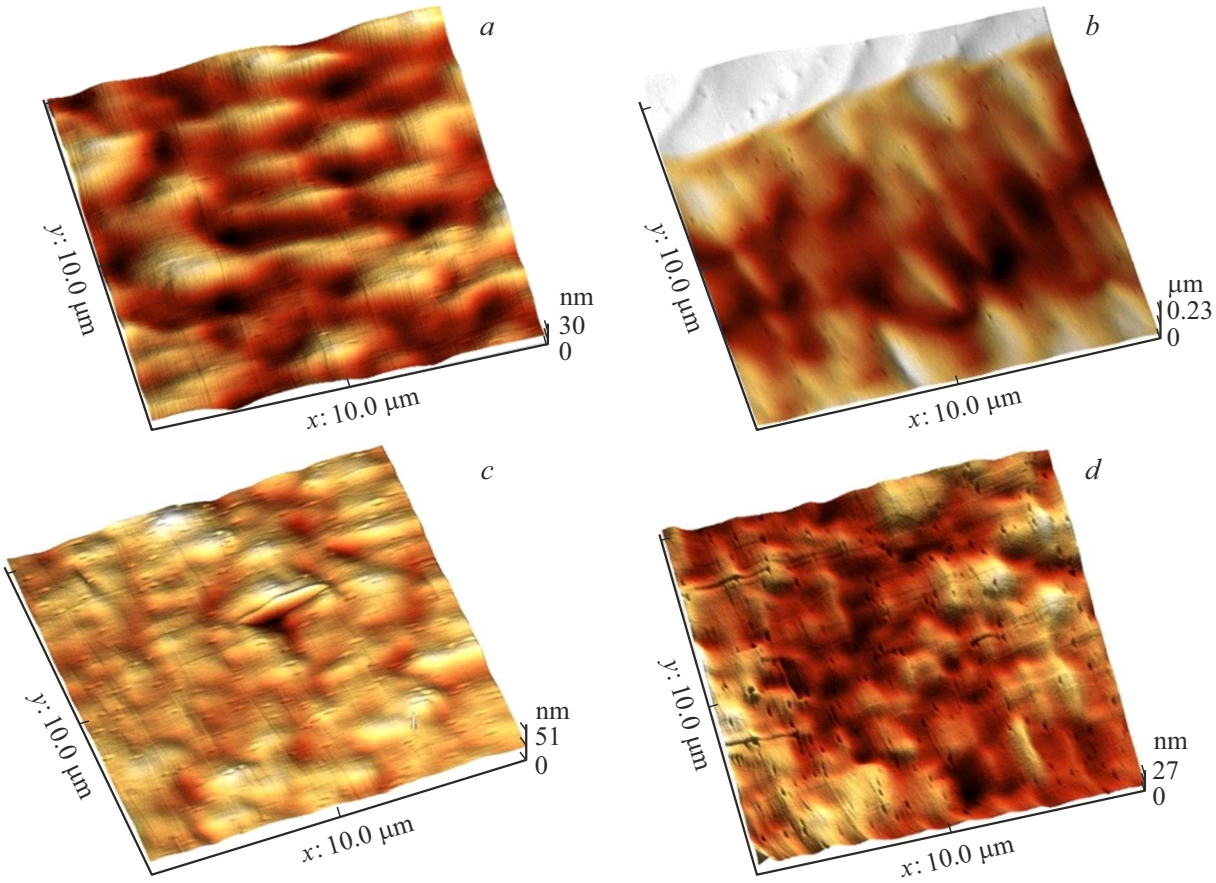

Figure 4. AFM images of the sample surface (scanning area $10\times10\,\mu m^2$) in the window center (*a* — sample 1, *c* — sample 2) and at the window edge (*b* — sample 1, *d* — sample 2).

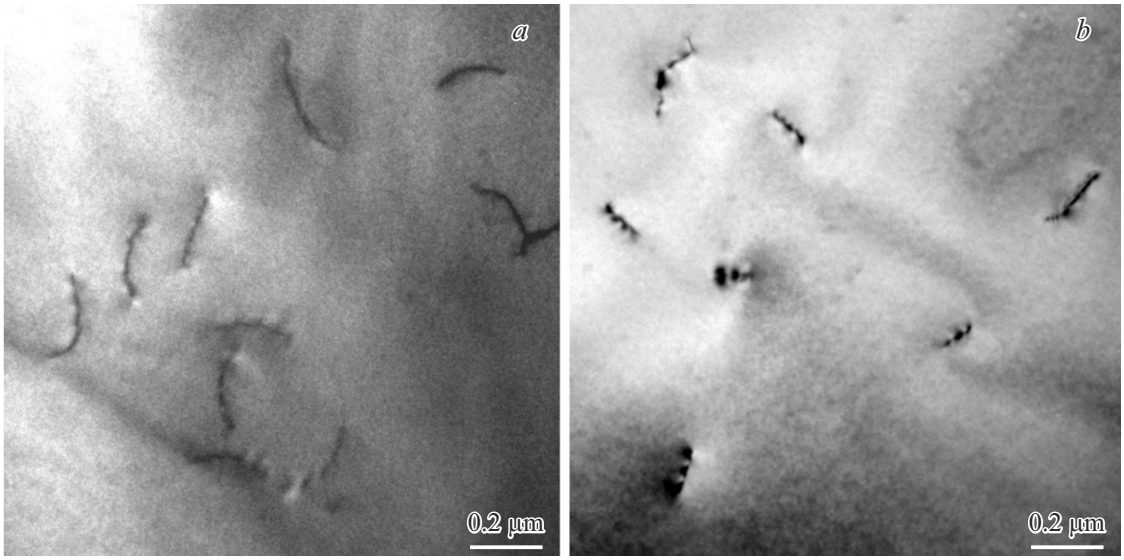

Figure 5. Light-field TEM-images of cross-sections in the planar geometry of a selectively grown GaAs layer in the central part of the window, obtained near the axis of zone [001]: *a* — sample 1, *b* — sample 2.

of optimized layers for radiators, amplifiers, modulators and photodetectors, which is impossible using standard epitaxy. This ability to control the layers thickness in one process is realized due to the window/mask geometry ratio, which makes it possible to obtain different wavelengths or absorption spectra in one technological process. At the same time, the absence of polycrystals on the mask allows for higher reproducibility and more accurate prediction of the parameters of selectively grown layers.

In order to quantify the root-mean-square roughness (RMSR) of the surface of a selectively grown GaAs layer, AFM studies of the surface morphology were performed. Figure 4 illustrates the AFM-images on the surface of $10\times10\,\mu$m in the center and at the window edge for samples 1 and 2. According to AFM-images the following values of RMSR wer obtained: for sample 1 its RMSR in the window's center was 4.87 nm and at the window's edge 8.3 nm, and for sample 2 RMSR in the window's center was 3.26 nm and at the edge — 3.92 nm. This behavior of RMSR may be explained by both the surface curvature and the thickness of the selectively grown layer. The thickness of the selectively grown layer and the thickness difference between the center and the edge of the window are noticeably greater for sample 1 than for sample 2 (see Figure 3). This can be indirectly confirmed by the fact that for a structure like 2 the RMSR of the pre-grown planar GaAs buffer layer on a Si substrate was ~ 2.5 nm.

To assess the defects of selectively grown GaAs layers of both types of samples, TEM was used to study the density of the growing-in dislocations (GID). Figure 5 shows light-field TEM images of the cross-sections in the planar geometry of selectively grown GaAs layers in the window's center, obtained near the axis of zone [001] for the near-surface region. GID dislocations were counted using 5 images with an area of $2\times2\,\mu\text{m}^2$: for sample 1 GID was in the range of $2.0-3.4\cdot10^8\,\text{cm}^{-2}$ and the averaged value was $\sim 2.9\cdot10^8\,\text{cm}^{-2}$; for sample 2 the GID stayed within $1.4-2.5\cdot10^8\,\text{cm}^{-2}$ and the averaged value was $\sim 2.1\cdot10^8\,\text{cm}^{-2}$. It can be seen from the data that GID values for 2 sample are less than for sample 1.

It should be noted that the results obtained have good reproducibility for both types of samples.

4. Conclusion

In this study, two types of GaAs samples were grown using the selective epitaxy method on a Si substrate: using SiO_2-mask directly on the surface of Si substrate (type 1 structure) and using SiO_2-mask on the surface of a planar GaAs buffer layer (type 2 structure). Based on the conducted research, the following differences in the main structural characteristics of the developed structures can be identified. Local changes of GID as observed by TEM method reached $2.0\cdot10^8$ and $1.4\cdot10^8\,\text{cm}^{-2}$ for the samples 1 and 2 respectively. The evaluation of the average value showed a difference of 1.5 times between the samples 1 and 2, which amounted to $2.9\cdot10^8$ and $2.1\cdot10^8\,\text{cm}^2$, respectively. Since the simplest GaAs-based buffers were used in the structures, the obtained GID values can be further reduced by using dislocation filters. Another important characteristic of the layers is the root-mean-square roughness of the surface, as it can affect the optical properties of quantum-dimensional active regions, leading to a broadening of the optical gain spectrum due to spatial thickness heterogeneity. The demonstrated values of RMSR in the center of the window were 4.87 and 3.26 nm for samples of type 1 and 2, respectively. The selective epitaxy is distinguished by a non-uniform growth rate over

the window area, which is also evident in our experiments. As a result, there is a heterogeneity in the thickness of the grown layers in the window, which leads to a stronger thickness difference over the window area with increasing layer thickness. So, for sample 1, with a thickness of the selectively grown layer in the window's center of 2410 nm, the difference in the thickness of GaAs layer between the central and extreme regions reaches 590 nm. A decrease in the thickness of the selectively grown GaAs layer for a type 2 sample to 800 nm resulted in lower difference in the thickness of GaAs layer between the center and the edge of the window to 110 nm. However, the influence of this effect can be mitigated by improving the design of the window and mask [13]. The modeling carried out in [13] showed that a decline in the non-uniformity of the growth rate in the window is possible by reducing the mask-to-window width ratio. In this case, the choice should be made within a tradeoff solution that takes into account the technologically acceptable minimum width of the mask and the density of the formed windows.

The conducted studies have shown the possibility of using various designs for the selective growth of bulk epitaxial layers on a silicon substrate (Figure 1). This allows the technology to be adapted to the specific requirements of the PIC fabrication process. For example, in the case of limitations caused by the growth of the polycrystalline phase on the mask surface, it is possible to implement a structure based on type 2 samples, when the buffer layer is formed before the growth of the emitting part and the fabrication of PIC other active and passive elements. However, if the technological process allows the presence of a polycrystalline phase, or it may be removed, then it is advisable to use the approach realized for a type 1 sample, since it allows reducing the number of technological operations.

Acknowledgments

The TEM studies were performed using the equipment of the Federal Joint Research Center „Materials science and characterization in advanced technologies," (Ioffe Physical-Technical Institute as a base organization) supported by the Ministry of Education and Science of the Russian Federation.

Conflict of interest

The authors declare that they have no conflict of interest.

References

[1] B. Wang, Y. Zeng, Y. Song, Y. Wang, L. Liang, L. Qin, J. Zhang, P. Jia, Y. Lei, C. Qiu, Y. Ning, L. Wang. Crystals, **12** (7), 1011 (2022). DOI: 10.3390/cryst12071011

[2] V. Shamakhov, S. Slipchenko, D. Nikolaev, A. Smirnov, I. Eliseyev, A. Grishin, M. Kondratov, I. Shashkin, N. Pikhtin. Nanomaterials, **13** (17), 2386 (2023). DOI: 10.3390/nano13172386

[3] X. Zhao, A.F. McKenzie, C.W. Munro, K.J. Hill, D. Kim, S.L. Bayliss, N.D. Gerrard, D.A. MacLaren, R.A. Hogg. J. Cryst. Growth, **603**, 127036 (2023). DOI: 10.1016/j.jcrysgro.2022.127036

[4] J. Decobert, G. Binet, A.D.B. Maia, P.-Y. Lagrée, C. Kazmierski. Adv. Opt. Techn., **4** (2), 167 (2015). DOI: 10.1515/aot-2015-0013

[5] A.P. Roth, P. Finnie, S. Charbonneau, C. Lacelle, C. Guerini, J. Fraser, M. Buchanan, Y. Feng. Microelectron. J., **28** (8–10), 909 (1997). DOI: 10.1016/S0026-2692(96)00130-9

[6] N. Morgan, V.G. Dubrovskii, A.-K. Stief, D. Dede, M. Sanglé-Ferrière, A. Rudra, V. Piazza, A.F. Morral. Cryst. Growth Des., **23** (7), 5083 (2023). DOI: 10.1021/acs.cgd.3c00316

[7] G. Afonso, G. Cerulo, N. Vaissiere, V. Vakarin, A. Elias, C. Fortin, J.-F. Paret, D. Lanteri, K. Mekhazni, F. Pommereau, J. Decobert. Phys. Status Solidi A, **221** (13), 2300656 (2024). DOI: 10.1002/pssa.202300656

[8] T. Fujii, K. Takeda, H. Nishi, N.-P. Diamantopoulos, T. Sato, T. Kakitsuka, T. Tsuchizawa, S. Matsuo. Optica, **7** (7), 838 (2020). DOI: 10.1364/OPTICA.391700

[9] V. Shamakhov, D. Nikolaev, S. Slipchenko, E. Fomin, A. Smirnov, I. Eliseyev, N. Pikhtin, P. Kop'ev. Nanomaterials, **11** (1), 11 (2021). DOI: 10.3390/nano11010011

[10] S. Slipchenko, V. Shamakhov, D. Nikolaev, E. Fomin, I. Soshnikov, A. Bondarev, M. Mitrofanov, N. Pikhtin, P. Kop'ev. Appl. Surf. Sci., **588**, 152991 (2022). DOI: 10.1016/j.apsusc.2022.152991

[11] S. Lourdudoss. Curr. Opin. Solid State Mater. Sci., **16** (2), 91 (2012). DOI: 10.1016/j.cossms.2012.01.003

[12] V. Shamakhov, S. Slipchenko, D. Nikolaev, I. Soshnikov, A. Smirnov, I. Eliseyev, A. Grishin, M. Kondratov, A. Rizaev, N. Pikhtin, P. Kop'ev. Technologies, **11** (4), 89 (2023). DOI: 10.3390/technologies11040089

[13] A.E. Marichev, V.V. Shamakhov, A.E. Grishin, S.O. Slipchenko, N.A. Pikhtin. FTP, **59** (8), 452 (2025). DOI: 10.61011/FTP.2025.08.62186.8457

Translated by T.Zorina